JOURNAL OF MATERIALS SCIENCE 7 (1972) 393–403

Investigation of the Aluminium-Aluminium Oxide Reversible Transformation as Observed by Hot Stage Electron Microscopy

C. A. GROVE, G. JUDD, G. S. ANSELL
Rensselaer Polytechnic Institute, Troy, New York, USA

Thin foils of high purity aluminium and an Al-Al_2O_3 SAP type of alloy were oxidised in a specially designed hot stage specimen chamber in an electron microscope. Below 450° C, amorphous aluminium oxide formed on the foil surface and was first detectable at foil edges, holes, and pits. Islands of aluminium then nucleated in this amorphous oxide. The aluminium islands displayed either a lateral growth with eventual coalescence with other islands, or a reoxidation process which caused the islands to disappear. The aluminium island formation was determined to be related to the presence of the electron beam. A mechanism based upon electron charging due to the electron beam was proposed to explain the nucleation, growth, coalescence, disappearance, and geometry of the aluminium islands.

1. Introduction

Recently it was shown that when thin foils of an Al-Al_2O_3 SAP type alloy were heated in an electron microscope, oxide growth started at the foil edges (including holes and pits) while islands of a second phase were observed to both form and disappear within the oxide [1]. Of particular interest in that study was the apparent reversibility in both the aluminium matrix to oxide reaction and the oxide to island reaction. However, no satisfactory mechanism for this reversibility was proposed.

In order to determine the nature of this rather unexpected event, it was the purpose of this investigation to observe if the above metal-oxide reactions also occurred in high purity aluminium and to determine a mechanism responsible for the reversibility. High purity aluminium was chosen as the investigating material since it was less complex than the two phase SAP alloy.

2. Material

The materials used for this investigation were:
1. High purity aluminium (99.999%), in the form of 18 in. ingots, supplied by United Mineral Co.
2. An Al-Al_2O_3 SAP type alloy, designation AT-400. The alloy contained 2.0 wt% γ-Al_2O_3 dispersed as irregular platelets approximately 600 Å in diameter and 150 Å thick in a matrix of commercial purity aluminium [2].

3. Experimental Technique

The high purity aluminium was formed into 0.01 to 0.012 in. sheet by cold rolling small blocks cut from the ingot. These sheets were then annealed in air for 20 min at 450° C. The SAP type alloy was recrystallised for 8 h at 540° C in air after it had been cold rolled into 0.01 in. strips from $\frac{1}{4}$ in. extruded rods.

Transmission samples for electron microscopy (less than 2000 Å thick) were prepared from the annealed sheets by standard electropolishing techniques [3]. The electrolyte used in both electropolishing techniques consisted of a solution of 20%, by volume, of perchloric acid in absolute ethanol at room temperature. In electropolishing several foils, a different electrolyte, consisting of 190 cc distilled water, 156 g chromic acid, 700 cc phosphoric acid, and 130 cc of sulphuric acid, was used to determine the effect, if any, of the type of thinning solution on the resulting oxidation reactions.

A special vacuum system was built into the specimen chamber of a Hitachi HU-11B electron microscope resulting in an ultimate pressure of 1×10^{-6} torr, an order of magnitude lower than usually obtained. This vacuum system consisted of a titanium sublimation pump and an ionisation gauge connected directly to the specimen chamber. In addition, a variable leak was attached to the back of the specimen chamber so that gas could be introduced into the chamber. Thus this system enabled the pressure to be varied from 1×10^{-6} to 9×10^{-4} torr in the region containing the sample. The thin foils were heated using a hot stage attachment in the modified electron microscope; here, temperature time and pressure were the variables studied.

To study the effect of the electron beam, three control experiments were performed. These control experiments consisted of variations in the sample heating and observation methods so as to determine the mechanism controlling the observed phenomena among the possible variables in the process. (Note that implicit in the term, observation, is that the electron beam is on the sample.)

These experiments were:

1. Heated in an external vacuum system, then cooled, then observed.
2. Heated in the electron microscope, then cooled, then observed, then reheated and simultaneously observed.
3. Heated in the electron microscope and simultaneously observed, then continued heating without observation, then cooled, then observed.

In addition, carbon films were placed on one side of several foils that were heated and directly observed in the hot stage electron microscope. Stereo pairs of foils that were heated and directly observed were also used in this investigation.

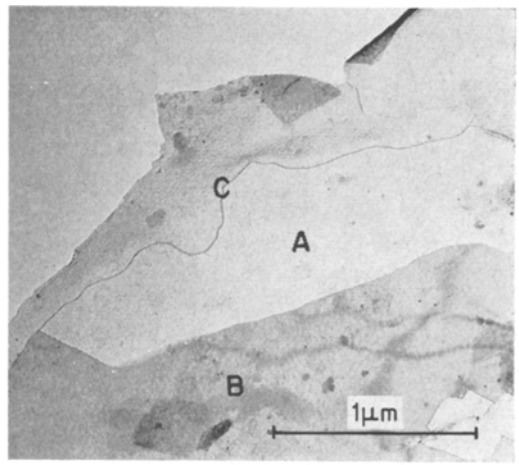

(a)

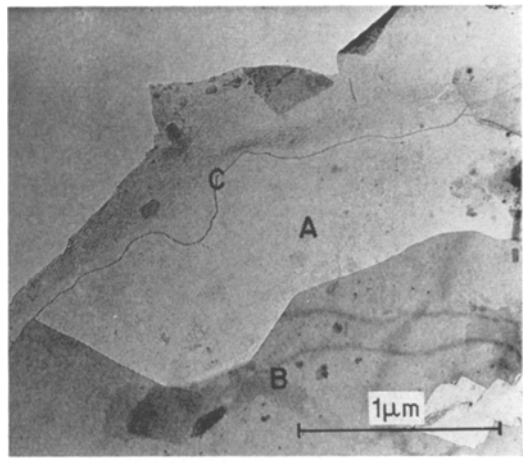

(b)

Figure 1 (a) Growth of white oxide at edge of a heated aluminium foil. Temperature 400°C. Pressure 5×10^{-6} torr. (b) Same area as in fig. 1a but 5 sec later. Note that the oxide-aluminium matrix interface has moved.

4. Results

4.1. Identification of Reaction Products in High Purity Aluminium and SAP AT-400

In the temperature range 100 to 450°C, the high purity aluminium when heated and simultaneously observed in the hot stage electron microscope, oxidised first at foil edges (figs. 1a and b). Region A is the oxide and region B is the aluminium matrix. It should be noted that the oxide-aluminium interface has advanced inward in fig. 1b. When the oxidation process stops and then starts again, a line is left at the points of the oxide-aluminium interface where movement has ceased. Such a line is shown in figs. 1a and b at C.

Soon after this initial oxide formation, small islands of a second phase began to appear and in some cases disappear inside this newly formed oxide. This is shown in figs. 2a, b and c; D is a second phase island, E is the oxide, F is the aluminium matrix, and C is the oxide-aluminium interface. Island A in fig. 2a can be seen to be growing in figs. 2b and c while island B in fig. 2a can be seen to be shrinking in figs. 2b and c. Note also that the oxide-aluminium interface C has moved. As these islands grew they coalesced and moved together in a liquid like motion reminiscent of Pashley's work on evaporated films [4]. The island growth and movement was most

active near the oxide-aluminium interface. Usually there existed a narrow zone, free of island material, at the oxide-aluminium interface.

The selected area diffraction pattern of the light appearing oxide in fig. 1 is shown in fig. 3. This diffraction pattern indicated that the initial oxide formed was amorphous. This diffraction pattern does contain diffuse haloes that become more pronounced as the time of oxide exposure to the electron beam increases. These haloes result from the crystallisation of the amorphous aluminium oxide into crystalline aluminium oxide by the electron beam. This effect has been previously illustrated by Suito *et al* [5] and Aladjem *et al* [6]. In addition to the diffraction results, the fact that the oxide had light contrast and that no defects or contours were observed in this area over a wide range of tilt and rotation of the specimen relative to the beam gave support to the argument that it was amorphous.

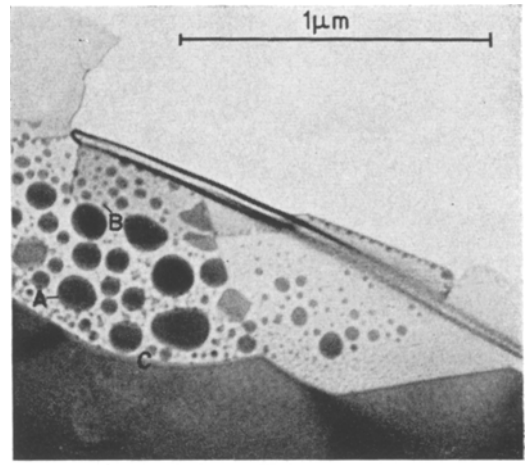

(c)

Figure 2 (a) Oxidised aluminium foil showing presence of islands within the white oxide. Temperature 430°C. Pressure 2×10^{-5} torr. (b) Same area as fig. 2a but 10 sec later. (c) Same area as fig. 2b but 10 sec later.

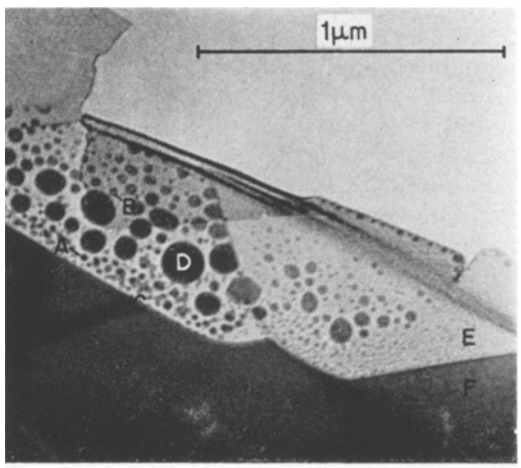

(a)

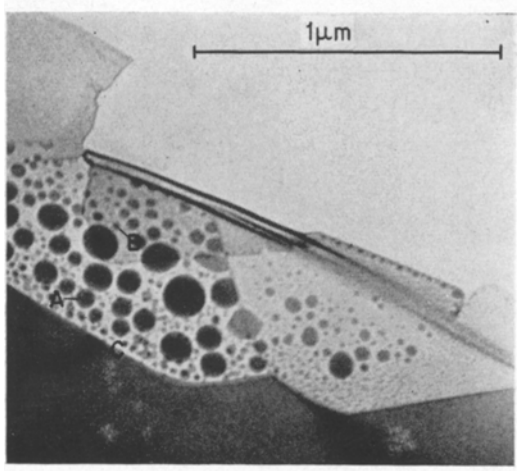

(b)

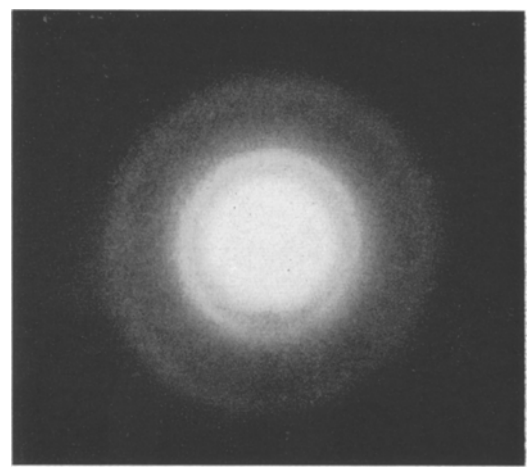

Figure 3 Selected area diffraction pattern of white aluminium oxide (fig. 1).

The selected area diffraction pattern of the second phase island material shown in fig. 2 is given in fig. 4. This diffraction pattern contains diffracted beams arising from three sources. These are (1) the aluminium matrix, (2) the amorphous oxide, and (3) the islands. The intense spots such as A and B are from the aluminium matrix. The spotted diffracted rings are from the islands and the amorphous oxide

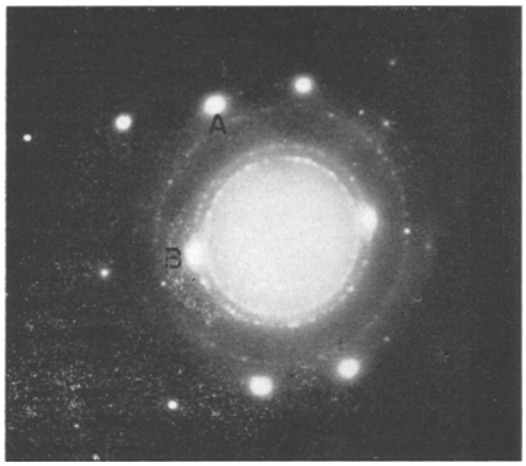

Figure 4 Selected area diffraction pattern of the islands (fig. 2).

TABLE I Comparison of calculated *d*-spacings from fig. 4 with known *d*-spacings for aluminium.

Ring number	Calculated *d*-spacings (A°)	*d*-spacings for [7] aluminium (A°)
1	2.35	2.34
2	2.05	2.02
3	1.43	1.43
4	1.20	1.22
		1.17
		1.01
5	0.92	0.93
		0.91

yields no diffraction spots. In solving this diffraction pattern, a gold standard was used to calculate the camera constant. Using this constant, the diffraction spots from the aluminium matrix (single crystal) were identified. Once the diffracting planes in the aluminium matrix were known, a more accurate camera constant could be calculated using aluminium as an internal calibration. Table I shows the *d*-spacings for the spotted diffraction rings due to the islands and compares them to the *d*-spacings for pure aluminium as determined from X-ray powder diffraction data [7]. It can be seen from table I that the island material is aluminium. The islands of aluminium are oriented randomly to one another since their diffraction pattern consisted of spotted diffraction rings.

These results disagreed with previous identification [1] of these two phases for an oxidised Al-Al_2O_3 SAP type alloy. Because of this disagreement, similar experiments were repeated using the SAP AT-400 alloy. Oxidised thin foils of the SAP AT-400 yielded the same phase transformation as the oxidised thin foils of aluminium. Thus the oxidation of both of these thin foils resulted in the nucleation and growth (or disappearance) of aluminium islands in a matrix of amorphous aluminium oxide. These observations were also independent of the electropolishing solutions employed.

4.2. Determination of the Cause of the Aluminium Island Formation

The results of the control experiments showed that the aluminium island formation within the oxide was associated with exposure to the electron beam during oxidation.

When the sample was heated in an external vacuum system (experiment 1) only amorphous aluminium oxide formed at the foil edges. No islands of aluminium were visible in the amorphous oxide.

Similar results were obtained when the samples were heated in the microscope without the electron beam on (experiment 2).

In addition, upon reheating the foil to temperature with the electron beam now on, new amorphous oxide was seen to have grown adjacent to the previously formed amorphous oxide and aluminium islands appeared within this newly grown amorphous oxide (fig. 5). No aluminium islands formed in the previously

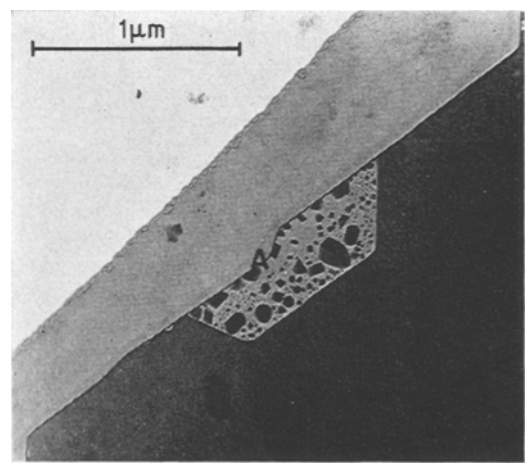

Figure 5 Aluminium foil which has been oxidised for 1½ h with the electron beam off; then reheated with the electron beam on. Note no aluminium islands are visible in the previously formed amorphous aluminium oxide but are present in the region of new oxide growth. Temperature 430° C. Pressure 5×10^{-6} torr.

formed or old amorphous oxide. This indicated that a moving oxide-aluminium interface, i.e. continued oxidation of the aluminium foil was necessary for the growth of aluminium islands. The aluminium islands did not grow past the boundary line (A) between the old amorphous oxide and the new amorphous oxide.

Electron diffraction patterns of the old amorphous oxide formed with the beam off and the new amorphous oxide formed with the electron beam on were compared to see if any change in structure could be observed between the two amorphous oxides. No differences between the electron diffraction patterns could be noted.

Heating the sample after island formation without the electron beam on (experiment 3), showed that the aluminium islands could be oxidised, and thus tended to disappear when the electron beam was removed from the sample (figs. 6a and b). The aluminium islands that did not oxidise were apparently protected by contamination of the foil surface by hydrocarbon deposition.

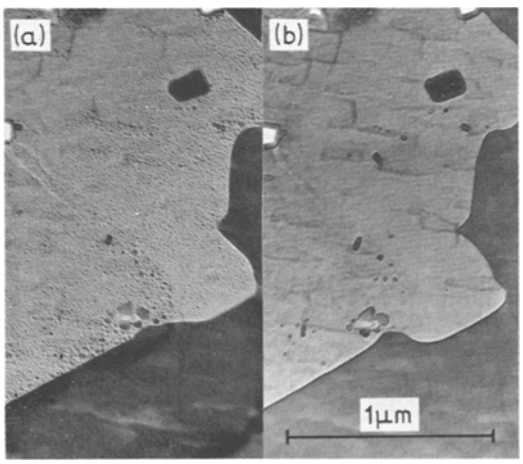

Figure 6 (a) Oxidised aluminium foil with aluminium islands in amorphous aluminium oxide formed with the electron beam on. (b) Same area as in (a), but the sample has been heated for an additional 70 min with the electron beam off. Note that most of the aluminium islands have disappeared. Temperature 400° C. Pressure 5×10^{-6} torr.

In order to see if these transformations were caused by the evaporation of aluminium from the aluminium matrix and its subsequent condensation on the amorphous oxide due to a thermal gradient created by the electron beam, a carbon film was placed on one side of a high purity aluminium foil. The foil was then heated *in situ* in the electron microscope at a temperature of 375° C and a pressure of 4×10^{-6} torr. No aluminium islands formed on the carbon film. This is in agreement with fig. 5 which showed no islands in the old amorphous oxide. Thus evaporation and condensation could be eliminated as a possible cause of these observations. Stereo pairs were taken to see if the aluminium islands were on the surface or if they were internal within the aluminium oxide. If the islands were on the surface, high surface diffusion caused by a thermal gradient created by the electron beam could account for the phenomena. The stereo pairs showed that the aluminium islands were located internally within the amorphous oxide and that they were thin platelets oriented parallel to the foil surface. Rapid surface diffusion therefore could also be discounted as a possible mechanism for this system.

4.3. Additional Experimental Observations

In most samples the amorphous oxide-aluminium interface moved in an oriented manner with respect to the aluminium matrix such that the aluminium oxide-aluminium interface line can be defined by a crystallographic direction of the aluminium matrix. This is well illustrated in figs. 1b and 5. Fig. 7a shows the oriented nature of the amorphous oxide-aluminium interface. Fig. 7b is the diffraction pattern of fig. 7a which includes diffraction from both the amorphous oxide and the aluminium matrix. Line AB was a macroscopic growth direction while line HD was the trace of the contact plane at the oxide-aluminium interface. From analysis of the diffraction pattern (correcting for image rotation due to intermediate and projector lenses) the growth direction AB was found to be the $\langle 1\,1\,0 \rangle$ direction and the contact or habit plane HD was a $\{1\,1\,0\}$ plane. The microscopic growth of the amorphous oxide occurred by forming a ledge or step at the oxide-aluminium interface. This step then moved along the interface consuming the aluminium matrix. The ledge motion was parallel to line HD and was thus also in the $\langle 1\,1\,0 \rangle$ direction.

Other low index planes of contact at the oxide-aluminium interface were present. Line EF was the trace of a $\{1\,0\,0\}$ plane of contact. Amorphous aluminium oxide growth occurred along this contact plane by forming a ledge (region G) which then moved down the interface in a $\langle 1\,0\,0 \rangle$ direction.

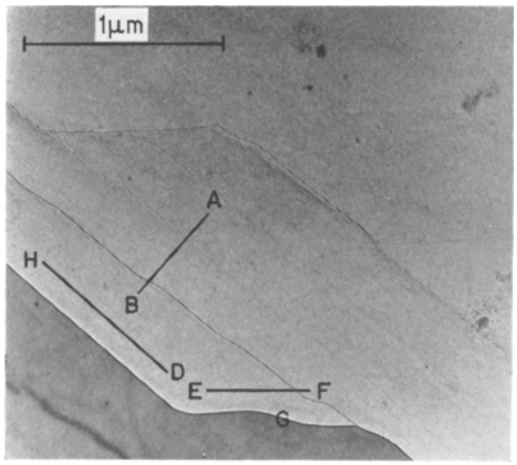

(a)

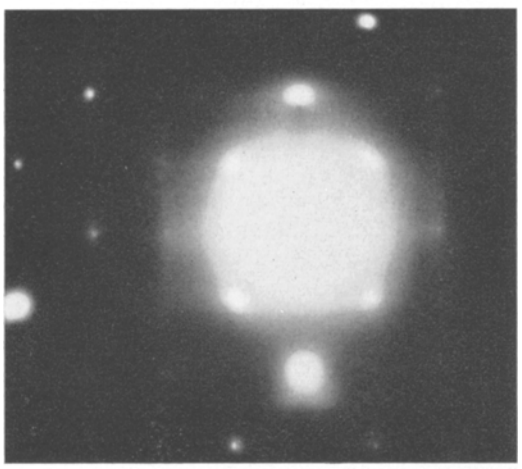

(b)

Figure 7 (a) Oxidised thin foil of aluminium showing the oriented nature of the amorphous aluminium oxide-aluminium matrix interface. Temperature 400° C. Pressure 6.5×10^{-6} torr. (b) Selected area diffraction pattern of fig. 7a.

For other aluminium foils heated *in situ* and simultaneously observed, oxygen was bled into the specimen chamber to increase the pressure to 9×10^{-4} torr. However, no increase in the reaction rate was observed.

The amorphous oxide film thickness was determined in order to compare it to the width of the island-free zone and to determine an approximate value for the percentage of electrons captured by the oxide.

The thickness of a thin foil can be determined from extinction contours [3]. The foil thickness is equal to

$$t = n E_g(1 + w)^{\frac{1}{2}}$$

where t = film thickness, $n = 0, 1, 2, 3 \ldots$ for bright fringes $= \frac{1}{2}, 3/2, 5/2 \ldots$ for dark fringes, w = deviation from the Bragg angle, and E_g = extinction distance for operating h, k, l reflection.

Fig. 8a shows the presence of extinction contours at the edge of an aluminium foil. The selected area diffraction pattern of fig. 8a (fig. 8b) shows that a strong (022) reflection is operating. A dark field photomicrograph of the area in fig. 8a using the (022) reflection is shown in fig. 8c. The dark field picture shows the contours more clearly than bright field because it contains only image contrast caused by the operating (022) reflection.

The deviation from the Bragg angle, w, is equal to zero along line AB in fig. 8c. From a knowledge of the extinction distance for an (022) reflection (1057Å), [3] the thickness of the foil at point T can be determined as follows:

$$t = n E_g$$

where $n = \frac{1}{2}$ (first dark fringes), $E_g = 1057$Å, $t = (\frac{1}{2})(1057$Å$)$, and $t = 528.5$Å at point T.

Since the foil thickness at the foil edge is seen to be approximately zero the angle of the foil and the thickness at any point in the first extinction distance can be readily calculated. Thus the half-angle of the foil wedge is 0.6° along the line AB.

Fig. 9 shows amorphous oxide growth that has occurred in 24 min. Line LP is the distance from the edge that the oxide has reached; measured at the exact place where the foil thickness was determined. The foil thickness at point P can now be found by the use of similar triangles. The total thickness of the wedge at point P is 113Å.

5. Discussion

The growth of aluminium islands in the amorphous aluminium oxide matrix was due to the electron beam (figs. 5 and 6). There are two possible ways in which the electron beam could cause this: (a) beam heating (b) electron charging.

The amorphous aluminium oxide is a thermal insulator while the aluminium matrix is a thermal conductor. Since the amorphous aluminium oxide is unable to conduct away the energy absorbed from the electron beam, a thermal gradient across the oxide-aluminium interface is created. However, it is difficult to attribute the growth and disappearance of the aluminium

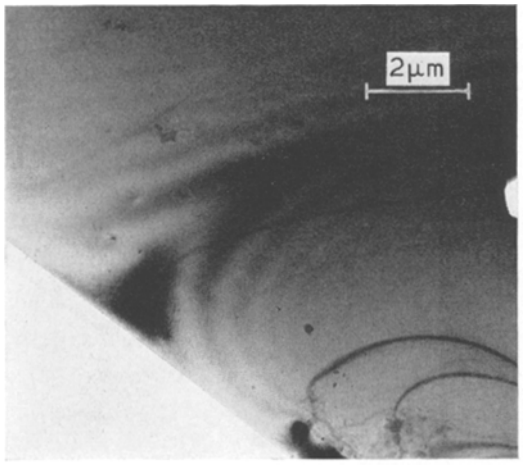

8(a)

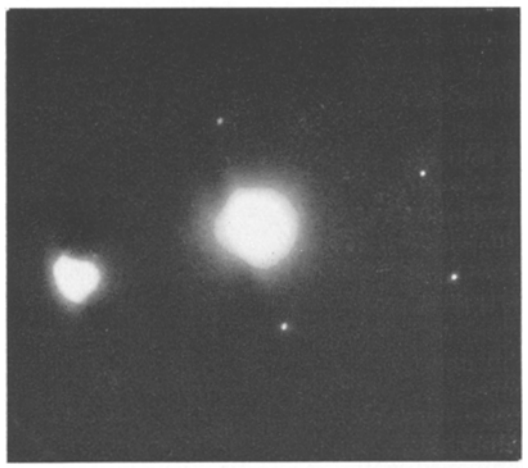

8(b)

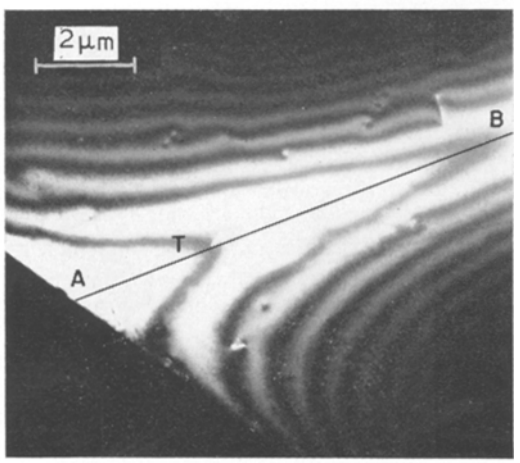

8(c)

Figure 8 (a) Extinction contours at the edge of an aluminium foil. (b) Selected area diffraction pattern of fig. 8a. Note the strong (022) reflection. (c) Dark field photomicrograph of fig. 8a showing extinction contours as seen using an (022) reflection.

islands to the presence of this thermal gradient. The mechanism of (1) rapid surface diffusion and (2) evaporation and condensation, which depend on a thermal gradient, have been discounted by experimental observations mentioned in the previous section.

Electron charging involves the capture of electrons from the electron beam and their subsequent recombination with aluminium ions to form aluminium islands. Electron charging is a mechanism that is consistent with the experimental observations and will be discussed in the succeeding paragraphs.

5.1. Amorphous Aluminium Oxide Formation

Below 450°C, amorphous aluminium oxide forms on the aluminium surface by the diffusion of aluminium ions to the outer surface to meet with oxygen ions [8-10]. The rate of oxidation is temperature sensitive, and increases with increasing temperature. Because the diffusing species is aluminium ions, a concentration gradient of aluminium ions exists in the amorphous aluminium oxide. The concentration of aluminium ions is greatest at the oxide-aluminium interface [11]. As the oxidation process continues

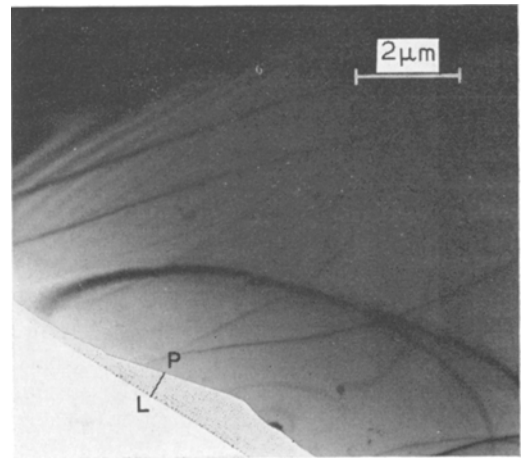

Figure 9 Amorphous oxide growth in the same area as fig. 8c during 24 min. Temperature 400°C. Pressure 3×10^{-6} torr.

the amorphous aluminium oxide becomes visible at thin areas in the foil (edges, holes, etc.), since in these regions all of the aluminium matrix has oxidised (fig. 10). Once the amorphous oxide is visible, its growth can be followed by noting the movement of the oxide-aluminium interface. The amorphous oxide-aluminium interface grows in an oriented manner with respect to the aluminium matrix in most observed cases. A common plane of contact at the oxide-aluminium interface is a {110} plane and the growth direction is ⟨110⟩. The oxide-aluminium interface appears to advance by forming a ledge or step at the interface which then sweeps across the interface.

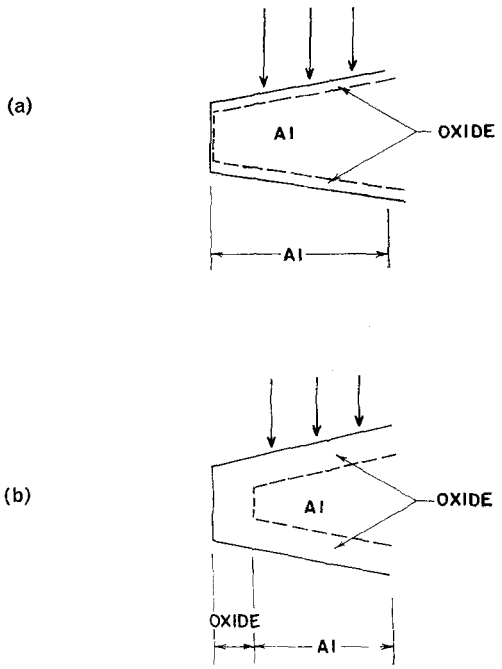

Figure 10 (a) Amorphous aluminium oxide covering the surface, but not yet visible. Time t_1. (b) Amorphous aluminium oxide now visible. Time $t_2 (t_2 > t_1)$.

5.2. Nucleation and Growth of the Aluminium Islands

The amorphous aluminium oxide is an electrical insulator as compared to the aluminium matrix. As electrons from the electron beam pass through the amorphous aluminium oxide, a small percentage of them are captured. It has been estimated that in thin foils suitable for transmission electron microscopy (1000Å) approximately 1% of the beam is absorbed [12]. Since the amorphous aluminium oxide is an insulator, it retains the charge imparted to it by the electron beam and becomes negatively charged. When several of these captured electrons are within a given volume, a localised electric field exists (fig. 11). As an example of this type of electron concentration effect, Chopra [13] has used electron beam charging in his experiments on the growth of thin evaporated metal films.

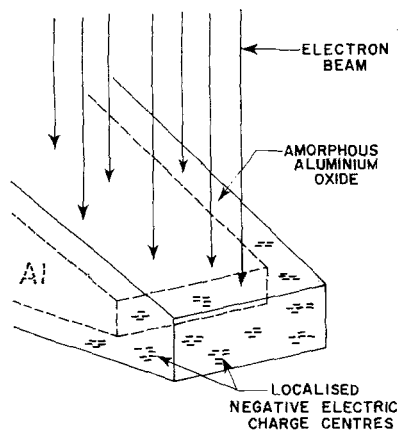

Figure 11 Illustration showing the formation of localised negative electric charge centres in the amorphous aluminium oxide by the electron beam.

As the diffusing aluminium ions approach the negatively charged electric field centres, the ions are attracted to them. When the aluminium ions reach these negative field centres, they recombine with the centres to form nuclei of neutral aluminium. As the electrons in the beam continue to pass through the amorphous aluminium oxide and existing aluminium nuclei, not only are new nuclei formed, but also the existing aluminium nuclei become negatively charged since the aluminium nuclei are completely surrounded by an insulator. Aluminium ions diffusing to the surface are atttracted to, and migrate toward these new negatively charged aluminium nuclei causing the aluminium nuclei to grow. This process occurs most rapidly near the aluminium matrix-amorphous oxide interface since the concentration of aluminium ions is greatest there.

A small island-free zone exists in the amorphous oxide next to the oxide-aluminium interface at most times. A possible explanation for this band could be that captured electrons in the zone, tunnel, or diffuse, to the aluminium

matrix thus preventing the formation of any aluminium islands.

5.3. Use of Electron Changing to Explain Experimental Observations

5.3.1. Aluminium Island Geometry

The percentage of the captured electrons in an oxide film 200Å thick needed to cause the growth of a rapidly growing aluminium island was calculated to be approximately 27% assuming 0.2% of the transmitted beam is captured in this foil thickness. This was determined using island A in figs. 2a, b and c which grew at a rapid rate. The percentage calculated represents an upper limiting value for this process (See appendix).

No aluminium islands were observed to be located in the amorphous oxide over the aluminium matrix. The amorphous oxide over the aluminium matrix is less than 100Å thick as was shown earlier. Electrons captured in the amorphous oxide over the aluminium have a high probability of being transported to the aluminium matrix because of the short diffusion distance involved. This argument is supported by the presence of an island-free zone, 100 to 400Å in width, next to the amorphous oxide-aluminium interface indicating that excess electrons, within a distance of approximately 100Å, probably discharge to ground through the aluminium matrix.

Stereo pairs taken of the aluminium islands showed that they were thin platelets which were oriented perpendicular to the electron beam. This could be explained on the basis of electron charging by the fact that the energy of a charged particle is different from the energy of a neutral particle. In order to minimise this energy difference, excess electrons in a particle will move as far away as possible from one another, reducing their repulsive force. For instance, a spherical droplet of mercury will become an oblate spheroid when it is charged [13]. Since the aluminium islands are negatively charged, they will tend to have a geometrical shape which allows the electrons to be separated the greatest distance for a given volume. A thin platelet fits this requirement. The orientation of the aluminium platelets parallel to the foil surface could be explained by the direction of the aluminium flux away from the amorphous oxide-aluminium interface. This flow or flux of aluminium occurs parallel to the foil surface. Since the aluminium islands are fed by this flux, they would tend to grow parallel to the foil surface.

5.3.2. Aluminium Island Reversibility

The charge distribution on an aluminium island platelet is such that the electrons are located at the edges of the platelet [14]. This negative charge causes a flux of aluminium ions to the edge of the particle due to electrostatic attraction. Occurring simultaneously with the above process is the oxidation reaction which results in a flux of aluminium ions away from the island (fig. 12).

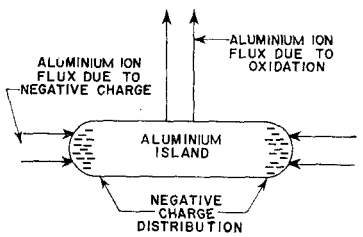

Figure 12 Illustration showing the aluminium ion flux due to both recombination and oxidation.

The fact that the aluminium islands continue to oxidise is proven by their disappearance when heated with the electron beam off. The growth or disappearance (reversibility) of an aluminium island depends on the relative rates of these two processes. If the oxidation rate is greater than the rate of incoming aluminium ions, the aluminium island will disappear. If the incoming rate of aluminium ions is greater than the flux of aluminium ions away from the island due to oxidation, the aluminium island will grow. These processes, of course, depend on the rate of electron capture and on the availability of aluminium ions in the vicinity of the islands.

5.3.3. Aluminium Island Coalescence

As the aluminium islands grow, many of them coalesce with one another and in doing so move in a liquid-like manner. A similar observation of coalescence and liquid-like behavour of charged metallic nuclei, or islands, on nonconducting substrates has previously been observed. Chopra has shown that if two charged islands have a substantially different charge (independent of sign), there would be an attractive force between them to cause coalescence [13]. He also showed that the shear force caused by such a charge difference, once a small area of contact was made, would be sufficient to cause the liquid-like movement of the islands. Thus in the

present case, although the oxide provides a constraint to movement, the same type of inter-island forces should be present. If two islands have approximately the same negative charge, a repulsive force exists. These two islands can still coalesce. If the rate of aluminium ions entering the two islands is fast enough, the repulsive force can be lowered or eliminated temporarily and the distance between the islands shrinks. This continues until a neck is formed whereby the two islands have coalesced (fig. 13).

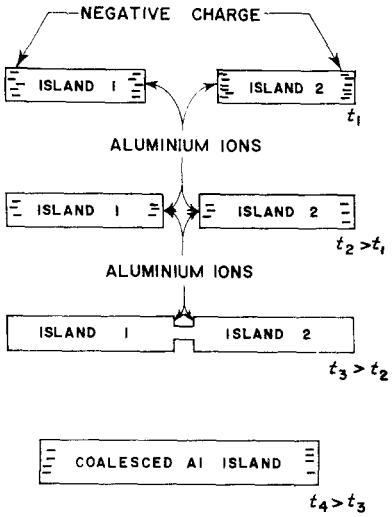

Figure 13 Illustration showing the coalescence of two aluminium islands.

5.3.4. Aluminium Island Contrast Change

During the growth of the aluminium islands, many of them change contrast. That is, the islands appear light grey for a period of time, then rapidly turn black followed by a return to light grey (figs. 2a, b and c). This change in island contrast can also be explained by the proposed electron charging theory. The islands that become entirely or partially black are ones that have become highly negatively charged. This causes the electrons in the electron beam to be deflected around the island, giving its black appearance. With the addition of new aluminium ions, the negative charge is reduced and the island returns to its normal contrast.

6. Conclusions

1. The phenomena of the precipitation reaction that is observed when high purity aluminium and SAP AT-400 is oxidised in the hot stage of an electron microscope consists of the nucleation and growth (or disappearance) of thin aluminium platelets within a matrix of amorphous aluminium oxide. The electron beam plays an integral role in the nucleation and growth of the aluminium islands.

2. A mechanism proposed to explain the formation of the aluminium island nuclei is the recombination of aluminium ions migrating to the surface with electrons from the electron beam captured in the amorphous aluminium oxide. These islands may grow by the further recombination of aluminium ions and the electron captured in the aluminium islands due to their being entrapped in an insulating amorphous aluminium oxide.

The reversibility of the aluminium islands may be caused by the competition of the recombination and oxidation processes. When the oxidation rate is more rapid, the aluminium island disappears. Coalescence of the aluminium islands may be by the attractive forces due to a difference in electron charge on the aluminium islands or by the speed of recombination to eliminate repulsive charge.

3. The oxidation process and the aluminium island formation is sensitive to temperature and electron beam intensity but insensitive to pressure in the range of 1×10^{-6} to 9×10^{-4} torr and to thinning solutions. These reactions increase with increasing temperature and electron beam intensity.

Acknowledgements

The work reported in this paper was supported by the Office of Naval Research and the National Aeronautics and Space Administration. The studies were conducted in the NASA Interdisciplinary Materials Research Centre at Rensselaer Polytechnic Institute.

The authors wish to thank Dr H. B. Huntington and Dr J. B. Hudson for their helpful discussions.

References

1. R. NATESH and G. S. ANSELL, *Acta Metallurgica* **14** (1966) 711.
2. R. S. GOODRICH JUN. and G. S. ANSELL, *ibid* **12** (1964) 1097.
3. P. B. HIRSCH, A. HOWIE, R. B. NICHOLSON, D. W. PASHLEY, and M. J. WHELAN, "Electron Microscopy of Thin Crystals" (Butterworths, London, 1967), pp. 25, 416, 496.
4. D. W. PASHLEY, Thin Films (A. S. M. Metals Park, USA, 1964), p. 59.
5. E. SUITO, M. SHIOJIRI, and H. MORIKAWA, *J. Appl. Phys.* **5** (1966) 1197.

6. A. ALADJEM, D. G. BRANDON, J. YSHALOM, and J. JAHAVI, *Electrochim. Acta* **15** (1970) 663.
7. A.S.T.M. X-ray Powder Diffraction Data File.
8. A. F. BECK, M. A. HEINE, E. J. CAULE, and M. J. PRYOR, *Corrosion Sci.* 7 (1967) 1.
9. J. E. BOGGIO and R. C. PLUMB, *J. Chem. Phys.* **44** (1966) 1081.
10. P. E. DOHERTY, *Mem. Sci. Rev. Met.* **62** (1965) 197.
11. M. A. HEINE and P. R. SPERRY, *J. Electrochem. Soc.* **112** (1965) 359.
12. G. JUDD, Doctorial Dissertation, Rensselaer Polytechnic Institute, Troy, New York, (1967).
13. K. L. CHOPRA, *J. Appl. Phys.* **37** (1966) 2244.
14. D. HALLIDAY and R. RESNICK, "Physics for Students of Science and Engineering" (John Wiley and Sons, New York, USA, 1963) p. 639.

Received 30 July and accepted 4 October 1971.

Appendix

The percentage of captured electrons can be calculated in the following fashion:

$$P = \frac{(z)\ (\pi r_2^2 T - \pi r_1^2 T)\ (\rho)\ N_0}{D\ \Delta t \left(\frac{F}{A}\right)(\bar{A})\ (w)\ (10^{-2})} \qquad (1)$$

where:

z = charge of aluminium ion = + 3 (maximum possible charge); r_2 = radius of aluminium island at $t_2 = 6.25 \times 10^{-8}$ m; r_1 = radius of aluminium island at $t_1 = 2.63 \times 10^{-8}$ m; T = thickness of aluminium island (assumed to be 15Å and to the constant during Δt); ρ = density of aluminium = 2.7 g/cm^3; N_0 = Avogadro's number = 6.023×10^{23} atoms/mole; D = grams of aluminium per mole = 26.98 g/mole; Δt = time change during growth of island A = 10 sec; F = number of electrons per second in the beam = 3.14×10^{12} electrons/sec (based on the assumption that the beam current equals 5×10^{-7} A) [12].

A = beam area = 4.41×10^{-11} m^2 (based on a value of 7.5 μm for the beam diameter); $\bar{A}$ = mean island area = 7.24×10^{-15} m^2; w = percent of electron beam captured by a thin foil = 0.2%.

Substitution of the above values into equation 1 yields:

$$P = 26.8\%.$$